Communication in Physical Sciences, 2025, 12(8):2363-2371

Investigation of Pressure Dependence of Lattice Dynamical Properties of Potassium Phosphide in Rocksalt Structure using First-Principles Method

Shedrack O. Ani*, C. M. I. Okoye, and A.N.C. Agboku
Received:24 August 2025/Accepted: 09 December 2025/Published: 13 December 2025
https://dx.doi.org/10.4314/cps.v12i8.15

Abstract: *First-principles calculations have been carried out to investigate the structural stability, lattice dynamical properties, and pressure-dependent phonon behavior of potassium phosphide (KP) in the rocksalt structure. The phonon dispersion relations, phonon density of states (PHDOS), and pressure dependence of phonon frequencies were computed using the linear response approach within the framework of density functional perturbation theory (DFPT). The results reveal that KP is most stable in the rocksalt ferromagnetic phase. The absence of imaginary phonon frequencies at the equilibrium lattice constant confirms its dynamical stability, which is maintained up to a pressure of 2.57 GPa. Furthermore, the phonon frequencies at the high-symmetry points L, Γ, and X exhibit quadratic dependence on pressure, showing an overall increase with compression. The calculated mode Grüneisen parameters for the longitudinal optical (LO) and longitudinal acoustic (LA) phonon branches at these points are positive, indicating that the phonon frequencies increase under applied pressure. These findings provide valuable insight into the lattice dynamics and pressure-induced behavior of KP in the rocksalt phase.*

Keywords: *Linear response method; structural stability; phonon frequencies; Quantum Espresso; Gruneisen parameter.*

Shedrack Okwudiri Ani*
Department of Physics and Astronomy,
University of Nigeria, Nsukka, Enugu 410001,
Nigeria.
Email: shedrack.ani.91800@unn.edu.ng
https://orcid.org/0009-0006-8854-9410

Chukwuemeka M. Ijeoma Okoye
Department of Physics and Astronomy,
University of Nigeria, Nsukka, Enugu 410001,
Nigeria.
Email: cmi.okoye@unn.edu.ng

Ada Chinweoke Agbogu
Department of Physics and Astronomy,
University of Nigeria, Nsukka, Enugu 410001,
Nigeria.
Email: ada.agbogu@unn.edu.ng

1.0 Introduction

Binary pnictide compounds AlP, AlAs, GaP, and GaAs are potentially fitting for spin injection in spintronic devices because of their half-metallic ferromagnetic property. It has been found that CaN, SrN, and BaN in their rock salt structure exhibit half-metallic ferromagnetism. This positions them as a more advantageous candidate for the production of half-metallic thin films on suitable substrates. Binary alkali-metal pnictide materials are notable technological materials; a combination of alkali metals with group-15 elements yields a category of interesting semiconductors (Friedrich et al., 2011). Hypothetical RbN and CsN binary alkali-metal pnictide compounds have been discovered to be half-metallic ferromagnets at diverse structures, and they show an integer magnetic moment of 2μB. Results also show that the half-metallicity continued in the zinc-blend (ZB) structure up to 20%% and 15% shrinking of the lattice parameter for RbN and CsN compounds, which gives the chance to epitaxially grow these compounds on an extensive range of semiconductors (Lakdja, 2013). NaN and KN, which are both binary alkali-metal pnictides,

have been discovered to be half-metallic in their rocksalt and zinc-blende structures, which makes them valuable for spintronic field application (Yan, 2012). First-principles full-potential linearized augmented plane-wave (FP-LAPW) and plane-wave pseudopotential (PWPP) methods have been employed to explore the electronic and magnetic characteristics of alkali metal pnictides with a rocksalt structure. Results revealed that five compounds with the rocksalt configuration LiN, NaN, KN, KP, and KAs exhibit half-metallic ferromagnetism characterized by a magnetic moment of 2μB, largely due to significant spin splitting of the anion p states contributing to the observed magnetic moment. Furthermore, they determined that the rocksalt arrangement is energetically more favorable than the ZB structure (Gao et al., 2009). A study on the bulk and (111) surface of MP (M = K and Rb) in a rocksalt configuration using first-principles methods showed that both bulk compounds act as half- metallic ferromagnets and possess considerable half-metallic band gaps. Greater stability of the bulk compounds KP and RbP in the rocksalt structure compared to those in the tetragonal structure has been demonstrated. Results also indicated that for both substances, the FM states are more stable than the non-magnetic states (Gao et al., 2015). In their analysis of the physical characteristics of bulk MP (M = Li, Na, and K) for energy applications, Waheed et al. (2024) found that the phonon spectra demonstrated dynamic stability of the compounds because they lacked imaginary frequencies. Studies on the dynamic stability of alkali-metal pnictide compounds have shown that KP compound is dynamically unstable in the CsCl, ZB and wurzite(WZ) configurations, but remains dynamically stable in the RS structure, indicating that synthesis of KP compounds may only be feasible in the RS structure (Kazemi, 2017).

High pressure is instrumental in the search for new materials with outstanding properties. Investigating how vibrational modes respond to pressure is significant, as changes in pressure can affect the phonon dispersion of a material. This understanding has practical implications across various fields. Such insights contribute to the creation of new materials with specific characteristics, improve the functionality of cur- rent materials, and enhance our understanding of material behavior in extreme environments. Additionally, studying the pressure dependence of vibrational modes is essential because residual strains during epitaxial growth can impact the accurate experimental measurement of phonon frequencies (Camacho et al., 2002; Yurtseven, 2013). Alves (2009) investigated the phonon frequencies and their response to pressure in MnAs and MnN through first-principles calculations, demonstrating that the phonon frequencies of both materials react significantly to the application of pressure. The vibrational modes of MnAs and MnN demonstrate this dependence on pressure, exhibiting a negative bowing effect, which intensifies as one transitions from a lower symmetry structure to a higher symmetry one. The vibrational characteristics of KP when subjected to pressure remain underexplored. There is a limited amount of both experimental and theoretical data on the pressure dependence of phonon frequencies available in the literature, which may provide insights for the successful development of ferromagnetic layers. In this study, we concentrated on examining how lattice dynamical properties of the KP compound in its rock- salt structural phase change with varying pressure, utilizing the linear response method of density functional perturbation theory. Fig. 1 shows the primitive unit cell of the rocksalt structure of our material.

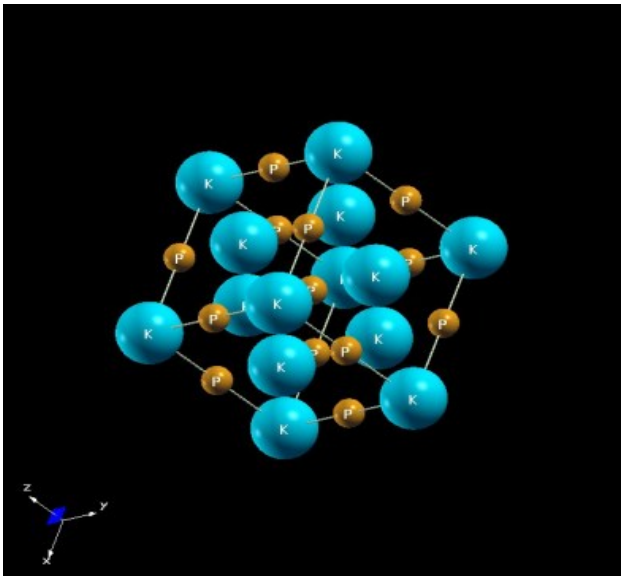

Fig. 1: Primitive unit cell of the rocksalt KP crystal structure, where the light blue spheres represent potassium atoms (K) and the yellow spheres represent the phosphorus atoms (P)

2.0. Computational Details

Potassium phosphide, KP, in the rocksalt structure, space group Fm$\bar{3}$m (225), has been studied in this work. The theoretical framework is the plane-wave density functional theory (PW-DFT) and the linear response method of density functional perturbation theory as implemented in the Quantum Espresso (QE) software (Giannozzi et al., 2009). The generalized gradient approximation (GGA) to DFT was used in the calculations for exchange-correlation correction. The estimated values of the plane-wave cutoff energy was determined to be 52Ry with ecutrho value of 520Ry, while the Brillouin zone sampling mesh parameters for the K-point were determined as 8 × 8× 8. The criterion of the energy convergence is set to $\Delta E \leq 10^{-4}$, where ΔE represents the difference in total energy between consecutive values. The equilibrium lattice parameter was found by fitting the obtained energy as a function of volume data to the Murnaghan equation of state (EOS) (Murnaghan, 1994). Fundamentally, a per- turbation in ionic positions gives the dynamical matrix, which is now used to calculate the frequency of the phonons:

$$F_l \equiv - \frac{\partial E_{BO}(R)}{\partial R_l} \quad (1)$$

Eq.(1) calculates the force constant matrix, which describes the interaction forces between atoms in a crystal (Baroni, 2010).

$$D_{sl}^{\alpha\beta}(\mathrm{q}) = \frac{1}{\sqrt{M_s M_l}} C_{sl}^{\widetilde{\alpha\beta}}(\mathrm{q}) \quad (2)$$

Eq.(2) calculates the dynamical matrix from the force constant matrix (Pavone et al., 1993).

$$\sum_s D_{sl}^{\alpha\beta}(\mathrm{q})\, u_{s\beta}(\mathrm{q}) = \omega^2 u_{s\alpha}(\mathrm{q}) \quad (3)$$

using Eq.(3), vibrational frequencies, ω, are determined by diagonalizing the dynamical matrix (Pavone et al., 1993). ω^2 are the eigenvalues of the 3n × 3n dynamical matrix, where n is the number of atoms in the unit cell. A q-mesh of 4 × 4 × 4 was employed for the density functional perturbation theory computations. By changing the unit cell volume and repeating the phonon frequency calculation process, the phonon frequency dependence on the applied pressure was determined. The pressure dependence of the phonon frequency is normally expressed in terms of the mode Gruneisen parameter (Pang et al., 2018). It elucidates the impact of pressure on a given material. The calculated mode Gruneisen parameters should capture the behavior of the phonon frequency reaction to the lattice change due to pressure (Pang et al., 2018). The evaluation of the Gruneisen parameter requires consideration of the pressure-induced shift in phonon frequencies (Yu et al., 2020). The mode Gruneisen parameter can be defined as (Talwar, 1990):

$$\gamma_i = \left(\frac{B_0}{\omega_0}\right) \frac{d\omega_i}{dP} \quad (4)$$

where $\frac{d\omega_i}{dP}$ is the frequency derivative of pressure, ω_0 is the phonon frequency at ambient pressure, B_0 is the bulk modulus, and γ_i is the ith mode Gruneisen parameter.

3.0 *Results and Discussion*

3.1 Structural stability properties

To determine the most stable phase of potassium phosphide (KP) in the rocksalt (RS) structure, we computed the total energy as a function of the lattice parameter for the ferromagnetic (FM), antiferromagnetic (AFM), and non-magnetic (NM) configurations. The calculations were performed using optimized parameters. The resulting total

energy values were fitted to the Murnaghan equation of state (Murnaghan, 1994), which yielded the equilibrium lattice constant (a_0), bulk modulus (B_0), and pressure derivative of the bulk modulus (B'), for each phase. The obtained parameters are summarized in Table 1.

Fig. 2 illustrates the variation of total energy with lattice parameter for the three magnetic phases of RS–KP. As shown, the ferromagnetic phase exhibits the lowest total energy, indicating that it is the most stable magnetic configuration of potassium phosphide in the rocksalt structure.

From Table 1, the ferromagnetic phase is the most stable, so it is used for all calculations in this study. It is also seen from Table 1 that in the ferromagnetic phase of the rocksalt structure, the equilibrium lattice constant is 12.9973 a.u. Table 1 shows that our results are in reasonable agreement with previous studies (Gao et al., 2009, 2015; Kazemi, 2017).

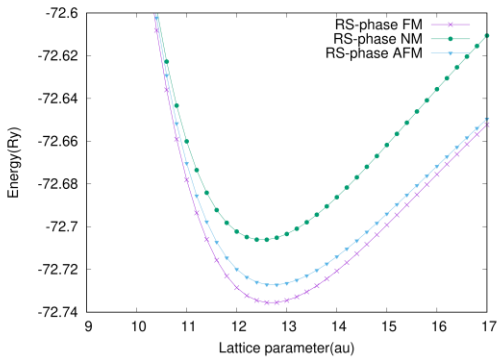

Fig. 2: Energy versus lattice constant curves for RS structure of KP compound in ferromagnetic (FM), anti-ferromagnetic (AFM) and non-magnetic (NM) phases.

3.2 Vibrational properties of the compounds

The lattice vibrational properties of potassium phosphide (KP) were calculated using the method outlined in Section 2. In subsection 3.2.1, the results of phonon dispersion spectra and the phonon density of states calculations were presented.

Table 1: Calculated equilibrium lattice constant, a_0, bulk modulus, B_0, and pressure dependence of bulk modulus, B′ , for KP compound in the RS structural phase

Compounds	a_0(a.u)	B_0(GPa)	B'
KP-FM	12.9973	9.6	3.42
	12.6042[1]		
	12.7290[2]		
	12.7660[3]		
KP-AFM	13.0230	9.0	3.45
KP-NM	12.7532	10.0	3.63

[1]Gao et al. (2009), [2]Gao et al. (2015), [3]Kazemi (2017)

3.2.1 Phonon frequency dispersion & density of states

The phonon dispersion spectra at the equilibrium lattice constant for the KP in the rocksalt structure are displayed in Fig. 3. The RS structure of the KP compound is dynamically stable, as evidenced by the lack of negative frequencies in its phonon spectrum. The FM state KP compound's phonon results in the RS phase are consistent with earlier findings (Kazemi, 2017; Waheed et al., 2024).

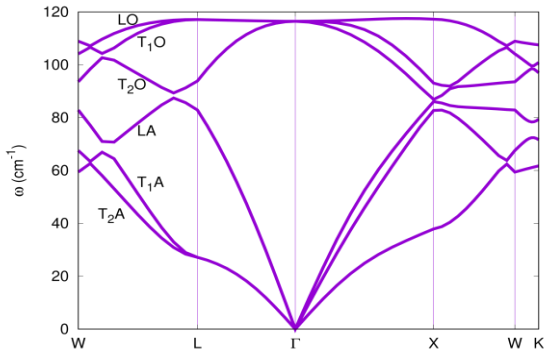

Fig. 3: Phonon dispersion of KP in rocksalt structure at equilibrium lattice constant (0 GPa)

The phonon dispersion of potassium phosphide (KP) in the rocksalt (RS) phase exhibits six distinct branches, spanning frequencies from approximately $0cm^{-1}$ to 117 cm^{-1}. This set of

six branches arises from the two atoms present in the unit cell, each con- tributing three vibrational modes, yielding a total of six phonon modes. The spectrum consists of three acoustic and three optical branches: the acoustic modes are characterized by zero frequency at the Γ point, while the optical modes exhibit non-zero frequencies at the same point. Specifically, the acoustic modes comprise two transverse acoustic branches (T_1A and T_2A) and one longitudinal acoustic branch (LA), whereas the optical modes include two transverse optical branches (T_1O and T_2O) and one longitudinal optical branch (LO). A clear longitudinal–transverse optical (LO–TO) splitting is observed at the high-symmetry points L and W, indicating the presence of polar interactions in the RS–KP lattice.

The phonon density of states (phonon-DOS) of the KP compound in the rocksalt structure is shown in Fig. 4. The KP phonon density of states shows no phonon distribution around the negative region of the frequency axis. The Fig. also shows the atom decomposed density of states, highlighting the contributions of potassium, K, and phosphorus, P atoms.

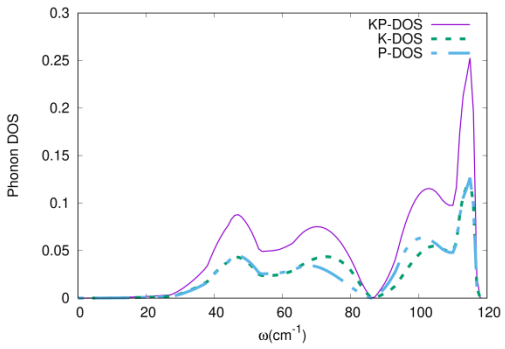

Fig. 4: Phonon density of states of KP in rocksalt structure showing the total KP phonon density of states and the atom decomposed contributions K-DOS and P-DOS at 0 GPa

Between $0\,cm^{-1}$ and $65cm^{-1}$, the total phonon density of states (phonon-DOS) arises due to nearly equal contributions from both K and P atoms. In the range of $65cm^{-1}$ to $85cm^{-1}$, The phonon-DOS is dominated by vibrations associated with the K atoms, whereas between $85cm^{-1}$ and $110cm^{-1}$, the main contribution arises from the P atoms. Above $110cm^{-1}$, the contributions from both K and P atoms become nearly equal again. This similarity in their contributions across certain frequency ranges is likely due to the closeness of their atomic masses.

3.3 Effect of pressure on phonon dispersion

The pressure (P) dependence of the KP phonon dispersion curves along selected high-symmetry directions in the Brillouin Zone (BZ) is presented in Fig. 5 & Fig. 6. With increasing pressure, most phonon branches shift toward higher frequencies. However, further increase in pressure cause some phonon modes to acquire negative frequencies, indicating a loss of dynamical stability of the KP compound in the rocksalt

(RS) phase. The structure becomes dynamically unstable at a pressure of approximately 2.57 GPa. Moreover, increasing pressure enhances the transverse optical–longitudinal optical (TO–LO) splitting near the L, X, and W points in the BZ. Consistent with the trends observed in Fig. 5 & Fig. 6, the overall magnitude of the phonon frequencies increases with pressure in the region where the compound remains dynamically stable (Kazemi, 2017; Xie et al., 1999).

Table 2 presents the phonon frequencies (ω) at the high-symmetry points L, Γ, and X as functions of pressure (P). Following the approach of Reparaz et al. (2018); Camacho et al. (2002), we fitted the data in Table 2 to a quadratic relation between the phonon frequencies and pressure, expressed as $\omega_s=\omega_0(cm^{-1}) + \frac{\partial\omega}{\partial P}(\frac{cm^{-1}}{GP_a}).P + \frac{\partial^2\omega}{\partial P^2}(\frac{cm^{-1}}{GP_a^2}).P^2$.

The fitted parameters ω_0, $\frac{\partial\omega}{\partial P}$, and $\frac{\partial^2\omega}{\partial P^2}$ are summarized in Table 3. Fig. 7 illustrates the quadratic fits of the calculated phonon modes. As pressure increases, the LO modes at L, Γ, and X points diverge, while the LA modes at L and X become degenerate around 1 GPa and subsequently separate at higher pressures. Interestingly, the phonon frequencies in the rocksalt (RS) structure exhibit an overall positive correlation with pressure for KP, indicating phonon hardening under compression.

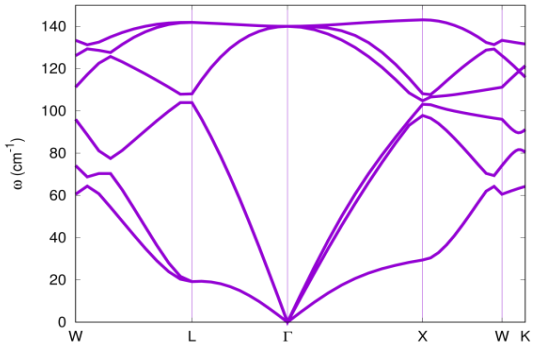

Fig. 5: Phonon dispersion curves of KP at P= 1.05 GPa

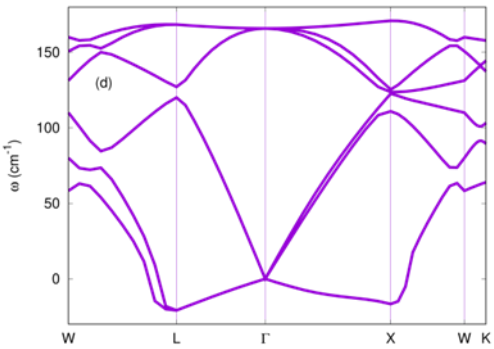

Fig. 6: Phonon dispersion curves of KP at P= 2.57 GPa

Table 2: Phonon frequencies (ω) (cm^{-1}) at high symmetry points L, Γ, and X as a function of pressure (P)(GPa)

P(GPa)	ω at L	ω at Γ	ω at X
	LA=79.3		LA=82.5
0.0	TA=22.9	LO=116.2	T_1A=77.7
	LO=116.7		$T_2A = 35.4$
	T_1O=116.7		LO=116.7
	T_2O=95.3		T_1O=94.5
			T_2O=89.6
0.48	LA=89.6		LA=91.9
	TA=21.3	LO=127.9	T_1A=86.5
	LO=129.1		T_2A=33.1
	T_1O=129.1		LO=129.6
	T_2O=102.3		T_1O=101.8
			T_2O=98.1
1.05	LA=102.1		LA=102.0
	TA=18.1	LO=140.3	T_1A=95.3
	LO=142.0		T_2A=29.1
	T_1O=142.0		LO=143.2
	T_2O=109.8		T_1O=109.1
			T_2O
=107.1			
1.74	LA=112.3		LA=113.8
	TA=10.9		T_1A=106.1
	LO=156.2	LO=153.9	T_2A=26.4
	T_1O=156.2		LO=157.5
	T_2O=117.7		T_1O=116.6
			T_2O=115.9
2.57	LA=122.9		LA=123.6
	TA=20.1		T_1A=114.4
	LO=169.6	LO=167.0	T_2A=-12.9
	T_1O=169.6		LO=172.1
	T_2O =127.9		T_1O=126.3
			T_2O=125.7

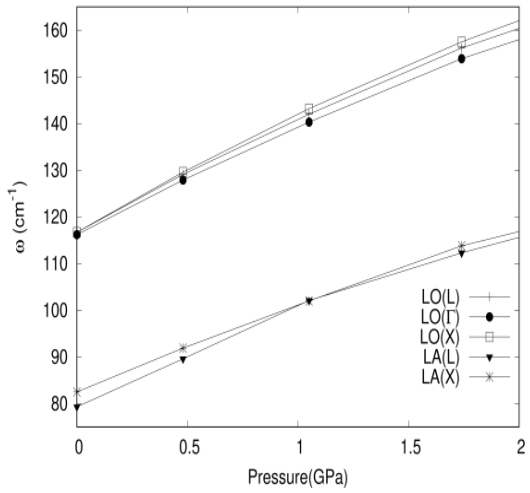

Fig. 7: Phonon frequencies of rocksalt KP at high symmetry points L, Γ, & X as a function of pressure. The points are calculated values while the curves are quadratic fits.

Table 3: Coefficients from the fits to the data in Figure 7 using

$$\omega_s = \omega_0(cm^{-1}) + \frac{\partial\omega}{\partial P}\left(\frac{cm^{-1}}{GP_a}\right).P + \frac{\partial^2\omega}{\partial P^2}\left(\frac{cm^{-1}}{GP_a^2}\right).P^2$$

Mode	$\omega_0(cm^{-1})$	$\frac{\partial\omega}{\partial P}\left(\frac{cm^{-1}}{GP_a}\right)$	$\frac{\partial^2\omega}{\partial^2 P}\left(\frac{cm^{-1}}{GP_a^2}\right)$
LO(L)	116.7 ±0.2	26.82 ±0.33	-2.421±0.123
LO(Γ)	116.2±0.1	25.39±0.25	-2.180±0.093
LO(X)	116.8±0.1	27.61 ±0.25	-2.376±0.093
LA(L)	79.2±0.6	24.09 ±1.18	-2.768 ±0.438
LA(X)	82.3 ±0.5	21.21±0.93	-1.976 ±**0.346**

3.3.1 The mode Gruneisen parameter

The results displayed in Table 4 show that the Gruneisen parameter (γ_i) of the LO phonon branch at the L, Γ, and X points in the Brillouin Zone, as well as for the LA branch, are all positive. The variations in the Gruneisen parameter at the various points in the BZ are small. This is consistent with the results of (Camacho et al., 2002) for ZnTe.

Table 4: Calculated Gruneisen parameters using $\gamma_i = \left(\frac{B_0}{\omega_0}\right)\frac{d\omega_i}{dP}$

Mode	$\omega_0(cm^{-1})$	$\frac{\partial\omega}{\partial P}\left(\frac{cm^{-1}}{GP_a}\right)$	γ_i
LO(L)	116.70	26.820	2.20
LO(Γ)	116.18	25.391	2.03
LO(X)	116.78	27.613	2.27
LA(L)	79.17	24.094	2.92
LA(X)	82.32	21.212	2.47

4.0 Conclusion

We investigated the phonon dispersion and its pressure response for potassium phosphide (KP) in the rocksalt (RS) structure using density functional theory (DFT) within the generalized gradient approximation (GGA), as implemented in Quantum ESPRESSO. The RS phase of KP is found to be ferromagnetically stable, consistent with previous reports (Gao et al., 2009, 2015; Kazemi, 2017).

Phonon dispersion calculations based on density functional perturbation theory (DFPT) reveal no imaginary frequencies, confirming the dynamic stability of the RS structure. The phonon spectrum spans 0 cm^{-1} to 117 cm^{-1}, comprising three acoustic and three de- generate optical branches. Phonon density of states analysis shows that both K and P atoms contribute nearly equally below 65 cm^{-1}, with K dominating between 65 cm^{-1} to 85 cm^{-1} and P between 85 cm^{-1} to 110 cm^{-1} ; above 110 cm^{-1}, their contributions are comparable.

Under pressure, most phonon branches shift to higher frequencies, but the extent varies across the Brillouin zone. Dynamic instability emerges at about 2.57 GPa, beyond which negative frequencies

appear, indi- cating that the RS phase cannot sustain higher pressures. The mode Grüneisen parameters for longitudinal optical and transverse acoustic modes exhibit varying pressure dependence. To our knowledge, no prior studies have reported Gru¨neisen parameters for rocksalt-type KP. We anticipate that our results will serve as a basis for future investigations.

Acknowledgments

Special thanks to my lecturers at the Department of Physics and Astronomy, University of Nigeria, Nsukka, where this work was done as part of M.Sc research

5.0 References

Alves, H. W. (2009). Phonons and their pressure dependence of MnAs and MnN by first-principles calculations. *Physica Status Solidi B, 246, 3, pp. 558–562.*

Baroni, S., Giannozzi, P., & Isaev, E. (2010). Thermal properties of materials from ab initio quasi-harmonic phonons. *Reviews in Mineralogy and Geochemistry, 71, pp. 39–57.*

Camacho, J., Loa, I., Cantarero, A., & Syassen, K. (2002). Vibrational properties of ZnTe at high pressures. *Journal of Physics: Condensed Matter, 14, 4, pp. 739–757.*

Friedrich, A., Winkler, B., Juarez, E. A., & Bayarjargal, L. (2011). Synthesis of binary transition metal nitrides, carbides and borides from the elements in the laser-heated diamond anvil cell and their structure–property relations. *Materials, 4, 10, pp. 1648–1692.*

Gao, G., Li, L., Xie, H., Lei, G., Deng, J., & Hu, X. (2015). First-principles study on bulk and (111) surface of MP (M = K and Rb) in rock-salt structure. *Materials Chemistry and Physics, 163, pp. 460–469.*

Gao, G., Yao, K., Liu, Z., Min, Y., Zhang, J., Fan, S., & Zhang, D. (2009). Bulk and surface sp half-metallic ferromagnetism in alkali metal pnictides with rocksalt structure: A first-principles calculation. *Journal of Physics: Condensed Matter, 21, 27.*

Giannozzi, P., Baroni, S., Bonini, N., Calandra, M., Car, R., Cavazzoni, C., Ceresoli, D., Chiarotti, G., Cococcioni, M., Dabo, I., de Gironcoli, S., Fabris, S., Fratesi, G., Gebauer, R., Gerstmann, U., Gougoussis, C., Kokalyj, A., Lazzeri, M., Martin-Samos, L., Marzari, N., Mauri, F., Mazzarello, R., Paolini, S., Pasquarello, A., Paulatto, L., Sbraccia, C., Scandolo, S., Sclauzero, G., Seitsonen, A., Smogunov, A., Umari, P., & Wentzcovitch, R. (2009). Quantum ESPRESSO: A modular and open-source software project for quantum simulation of materials. *Journal of Physics: Condensed Matter, 21, 39, pp. 395502.*

Kazemi, M., Amiri, P., & Salehi, H. (2017). Density functional study of d^0 half-metallic ferromagnetism in bulk and (001) nanosurface of KP compound. *Physics Letters A, 381, 30, pp. 2420–2425.*

Lakdja, A., Rozale, H., & Chahed, A. (2013). Half-metallic ferromagnetism in the hypothetical RbN and CsN compounds: First-principles calculations. *Computational Materials Science, 67, pp. 287–291.*

Murnaghan, F. D. (1944). The compressibility of media under extreme pressures. *Proceedings of the National Academy of Sciences of the United States of America, 30, 9, pp. 244–247.*

Pang, H. J., Chen, L. C., Cao, Z. Y., Yu, H., Fu, C. G., Zhu, T. J., Goncharov, A. F., & Chen, X. J. (2018). Mode Grüneisen parameters of an efficient thermoelectric half-Heusler. *Journal of Applied Physics, 124, 19, pp. 195102.*

Pavone, P., Karch, K., Schütt, O., Windl, W., & Strauch, D. (1993). Ab initio lattice

dynamics of diamond. *Physical Review B, 48, 5, pp. 3156–3163.*

Reparaz, J. S., Silva, K. P., Romero, A. H., Serrano, J., Wagner, M. R., Callsen, G., Choi, S. J., Speck, J. S., & Goñi, A. R. (2018). Comparative study of the pressure dependence of optical phonon transverse effective charges and linewidths in wurtzite InN. *Physical Review B, 98, 16, pp. 165204–165209.*

Talwar, D. N., & Vandevyver, M. (1990). Pressure-dependent phonon properties of III–V compound semiconductors. *Physical Review B, 41, 17, pp. 12129–12139.*

Vanderbilt, D. (1990). Soft self-consistent pseudopotentials in a generalized eigenvalue formalism. *Physical Review B, 41, 11, pp. 7892–7895.*

Waheed, H., Asghar, M., Ullah, H., Yaseen, M., Ali, A., Ibrahim, A., Laref, A., & Sharma, R. (2024). Computational insight into the physical properties of bulk MP (M = Li, Na, K) for energy applications. *ACS Omega, 9, 21, pp. 22831–22838.*

Xie, J., Chen, P., Tse, J., de Gironcoli, S., & Baroni, S. (1999). High-pressure thermal expansion, bulk modulus, and phonon structure of diamond. *Physical Review B, 60, 13.*

Yan, E. (2012). Half-metallic properties in rocksalt and zinc-blende MN (M = Na, K): A first-principles study. *Physica B: Condensed Matter, 407, 5, pp. 879–882.*

Yu, H., Huang, G., Peng, Q., Chen, L. C., Pang, H. J., Qin, X. Y., Qiu, P. F., Shi, X., Chen, L. D., & Chen, X. J. (2020). A combined experiment and first-principles study on lattice dynamics of thermoelectric $CuInTe_2$. *Journal of Alloys and Compounds, 822, pp. 153610.*

Yurtseven, H., & Tari, O. (2013). Calculation of the Raman frequencies as a function of pressure in the solid phases II and III (III′) of benzene. *Journal of Molecular Modeling, 19, pp. 2243–2248.*

Declaration

Consent for publication

Not Applicable

Availability of data and materials

The publisher has the right to make the data public

Ethical Considerations

Not applicable

Competing interest

The authors report no conflict or competing interest

Funding

The authors declared no source of funding

Author Contributions

Shedrack O. Ani conducted the first-principles calculations, performed data analysis, and drafted the manuscript. C. M. I. Okoye supervised the study, refined the methodology, and critically reviewed the work. A. N. C. Agboku assisted in data interpretation, validation of results, and manuscript revision. All authors approved the final manuscript.